Self-energy in surface electron spectroscopy: I. Plasmons on a free-electron-material surface

1998 J. Phys.: Condens. Matter 10 1733

(http://iopscience.iop.org/0953-8984/10/8/009)

J. Phys.: Condens. Matter **10** (1998) 1733–1751. Printed in the UK PII: S0953-8984(98)87358-X

Self-energy in surface electron spectroscopy: I. Plasmons on a free-electron-material surface

Z-J Ding†

CCAST (World Laboratory), PO Box 8730, Beijing, 100080, and Fundamental Physics Centre, University of Science and Technology of China, Hefei 230026, Anhui, People's Republic of China

Received 5 September 1997, in final form 8 December 1997

Abstract. On the basis of a quantum approach, the formula for the complex self-energy, and hence also that for the energy-loss cross-section, are derived for fast electrons penetrating through the surface from the interior of a solid. Both the angular and depth dependence are included in the expression. Use of a Drude–Lindhard model bulk dielectric function $\varepsilon(\boldsymbol{q}, \omega)$ for describing a bulk plasmon excitation in a free-electron-like material has yielded an analytical expression for the surface dielectric function which satisfies surface sum rules. The calculated imaginary and real parts of the electron self-energy for Si have indicated, in detail, the excitation processes of the surface plasmon and the bulk plasmon for an electron passing through the surface, with the dependency on electron energy and take-off angle. This approach provides quantitatively the electron inelastic scattering cross-section in the surface region for use in surface electron spectroscopy.

1. Introduction

Study of the inelastic scattering of electrons near a surface region is important to quantitative analysis by means of surface electron spectroscopy. Not only may the penetrating primary electrons incident on a target surface suffer inelastic scattering by the bulk and surface, but also so may the backscattering electrons escaping from the surface. This inelastic scattering contributes to single and multiple energy-loss peaks as well as the backscattering continuum. It is quite easy to see that the surface effect becomes more important with decreasing primary-electron-beam energy and increasing angle of incidence and take-off angle. In the same way, signal electrons generated in the bulk in Auger electron spectroscopy and x-ray photoelectron spectroscopy can have more chance to interact with the specimen surface because of the exponential decay behaviour of the intensity with the depth.

With a Monte Carlo technique, the multiple-scattering processes of electrons in a bulk material can be simulated quite well [1, 2], but an accurate and general description of surface excitation has been difficult to obtain, because most of the existing theories [3–10] concern only simple trajectory geometry, i.e., movement of the charge normal or parallel to the surface. Recently, several attempts [11–13] have been made to take account of surface effects in the treatment of electron inelastic scattering. However, in these models an averaging over electron trajectories has been carried out; it is thus not clear how the change between bulk excitation and surface excitation happens while an electron is crossing a surface.

† E-mail: zjding@nsc.ustc.edu.cn.

0953-8984/98/081733+19$19.50

In the first part of this paper (section 2) we shall adopt the quantum theory of Flores and Garcia-Moliner [14] to study the complex self-energy of charged particles on the surface. To make our development applicable to surface electron spectroscopy, we shall consider an important case, i.e. particles moving towards the surface from the interior of a bulk sample as well as escaping from a sample into the vacuum. The imaginary part of the complex self-energy gives directly the energy-loss cross-section that determines the energy-loss channels observed in surface electron spectroscopy. In section 3, a Drude–Lindhard model bulk dielectric function $\varepsilon(\boldsymbol{q},\omega)$ for describing a bulk plasmon is employed to derive analytically the surface dielectric function, which is shown to satisfy surface sum rules. As an example of the use of the calculation method, we obtain results for Si and demonstrate how we find the differential and total scattering cross-sections as functions of electron energy, direction of movement and distance from the surface. The effect of dispersion is also shown by comparing the result with that obtained using a dielectric function, $\varepsilon(\omega)$.

2. The electron self-energy

2.1. The calculation scheme

Let the specimen be described by a dielectric function $\varepsilon(\boldsymbol{q},\omega)$ and defined in a semi-infinite space, where $z<0$. The external charge at $\boldsymbol{r}=\boldsymbol{v}t$ moves with a velocity $\boldsymbol{v}=(\boldsymbol{v}_\parallel,v_\perp)$, where $v_\perp$ is positive for an electron approaching the surface from the bulk. We shall use the atomic units ($e=\hbar=m=1$) throughout. In the specular surface reflection model [15] the induced potential is determined by the external charge, its mirror image charge and the fictitious surface charges fixed by the boundary conditions [16, 17].

When the charge is in the vacuum ($z>0$), the total scalar potentials for the pseudovacuum ($z'>0$, where z' represents the field point) and the pseudometal ($z'<0$) are respectively [14]

$$\phi^{\mathrm{V}}(\boldsymbol{q},\omega)=\frac{4\pi}{q^2}\left\{2\cos(q_\perp z)+\sigma^+(\boldsymbol{q}_\parallel,\omega)\right\} \tag{1}$$

$$\phi^{\mathrm{M}}(\boldsymbol{q},\omega)=-\frac{4\pi}{q^2}\frac{\sigma^+(\boldsymbol{q}_\parallel,\omega)}{\varepsilon(\boldsymbol{q},\omega)} \tag{2}$$

where the surface charge determined by matching conditions at $z'=0$ is

$$\sigma^+(\boldsymbol{q}_\parallel,\omega)=-2\varepsilon_{\mathrm{s}}(\boldsymbol{q}_\parallel,\omega)\mathrm{e}^{-q_\parallel z} \tag{3}$$

with a surface dielectric function defined by

$$\varepsilon_{\mathrm{s}}^{-1}(\boldsymbol{q}_\parallel,\omega)=1+\frac{q_\parallel}{\pi}\int_{-\infty}^{\infty}\frac{\mathrm{d}q_\perp}{q^2\varepsilon(\boldsymbol{q},\omega)}. \tag{4}$$

The induced potential is obtained by removing the potential of the external charge

$$\Phi_{\mathrm{ind}}(\boldsymbol{q},\omega)=\phi(\boldsymbol{q},\omega)-\frac{4\pi}{q^2}\mathrm{e}^{-\mathrm{i}q_\perp z} \tag{5}$$

whose Fourier transformation to real z'-space yields

$$\Phi(z>0,z'>0)=\frac{2\pi}{q_\parallel}\mathrm{e}^{-q_\parallel(z+z')}\left\{1-2\varepsilon_{\mathrm{s}}(\boldsymbol{q}_\parallel,\omega)\right\} \tag{6}$$

$$\Phi(z>0,z'<0)=-\frac{2\pi}{q_\parallel}\mathrm{e}^{-q_\parallel z}\left\{\mathrm{e}^{q_\parallel z'}-2\varepsilon_{\mathrm{s}}(\boldsymbol{q}_\parallel,\omega)\frac{q_\parallel}{\pi}\int_{-\infty}^{\infty}\mathrm{e}^{\mathrm{i}q_\perp z'}\,\frac{\mathrm{d}q_\perp}{q^2\varepsilon(\boldsymbol{q},\omega)}\right\}. \tag{7}$$

When the charge is inside the metal, we have

$$\phi^{\mathrm{V}}(\boldsymbol{q},\omega) = -\frac{4\pi}{q^2}\sigma^{-}(\boldsymbol{q}_{\parallel},\omega) \tag{8}$$

$$\phi^{\mathrm{M}}(\boldsymbol{q},\omega) = \frac{4\pi}{q^2\varepsilon(\boldsymbol{q},\omega)}\left\{2\cos(q_{\perp}z) + \sigma^{-}(\boldsymbol{q}_{\parallel},\omega)\right\} \tag{9}$$

where

$$\sigma^{-}(\boldsymbol{q}_{\parallel},\omega) = -2\varepsilon_{\mathrm{s}}(\boldsymbol{q}_{\parallel},\omega)\frac{q_{\parallel}}{\pi}\int_{-\infty}^{\infty}\cos(q_{\perp}z)\ \frac{\mathrm{d}q_{\perp}}{q^2\varepsilon(\boldsymbol{q},\omega)}. \tag{10}$$

Then, for an isotropic dielectric function, $\varepsilon(\boldsymbol{q},\omega) = \varepsilon(q,\omega)$,

$$\Phi(z<0,z'>0) = -\frac{2\pi}{q_{\parallel}}\mathrm{e}^{-q_{\parallel}z'}\left\{\mathrm{e}^{q_{\parallel}z} - 2\varepsilon_{\mathrm{s}}(\boldsymbol{q}_{\parallel},\omega)\frac{q_{\parallel}}{\pi}\int_{-\infty}^{\infty}\mathrm{e}^{\mathrm{i}q_{\perp}z}\ \frac{\mathrm{d}q_{\perp}}{q^2\varepsilon(\boldsymbol{q},\omega)}\right\} \tag{11}$$

$$\Phi(z<0,z'<0) = \int_{-\infty}^{\infty}\mathrm{e}^{\mathrm{i}q_{\perp}z'}A(z|\boldsymbol{q},\omega)\ \mathrm{d}q_{\perp} \tag{12}$$

where

$$\begin{aligned}A(z|\boldsymbol{q},\omega) = {} & 2\mathrm{e}^{-\mathrm{i}q_{\perp}z}\left(\frac{1}{\varepsilon(\boldsymbol{q},\omega)} - 1\right)\frac{1}{q^2} + 2\mathrm{e}^{\mathrm{i}q_{\perp}z}\frac{1}{q^2\varepsilon(\boldsymbol{q},\omega)} \\ & - 4\varepsilon_{\mathrm{s}}(\boldsymbol{q}_{\parallel},\omega)\frac{q_{\parallel}}{\pi}\frac{1}{q^2\varepsilon(\boldsymbol{q},\omega)}\int_{-\infty}^{\infty}\mathrm{e}^{\mathrm{i}q_{\perp}z}\ \frac{\mathrm{d}q_{\perp}}{q^2\varepsilon(\boldsymbol{q},\omega)}.\end{aligned} \tag{13}$$

The three terms above explicitly display the origin of the bulk mode and the surface mode set up by an external charge. The first term describes the screening response of an infinite medium to the external charge and the second term that to the image charge. There is no bare Coulomb potential q^{-2} to be subtracted for the image charge term. The third one is due to the fictitious surface charges.

In time-ordered formalism, the RPA self-energy of a system inhomogeneous in the z-direction is written as

$$\Sigma(zz'|\boldsymbol{q}_{\parallel},\omega) = \mathrm{i}(2\pi)^{-3}\int\Phi(zz'|\boldsymbol{q}'_{\parallel},\omega')G_{\mathrm{s}}(zz'|\boldsymbol{q}_{\parallel}-\boldsymbol{q}'_{\parallel},\omega-\omega')\ \mathrm{d}\boldsymbol{q}'_{\parallel}\ \mathrm{d}\omega' \tag{14}$$

where G_{s} is the surface Green's function which can be constructed from a bulk free-electron Green's function.

2.2. Infinite barrier height

For a surface barrier of infinite height, an external charge should be reflected at the surface. The wave function of the moving electron is made up of incoming and outgoing plane waves. The surface Green's function is

$$\begin{aligned}G_{\mathrm{s}}(zz'|\boldsymbol{q}_{\parallel},\omega) &= G(z-z'|\boldsymbol{q}_{\parallel},\omega) - G(z+z'|\boldsymbol{q}_{\parallel},\omega) \\ &= (2\pi)^{-1}\int_{-\infty}^{\infty}G(\boldsymbol{q},\omega)(\mathrm{e}^{\mathrm{i}q_{\perp}(z-z')} - \mathrm{e}^{\mathrm{i}q_{\perp}(z+z')})\ \mathrm{d}q_{\perp}\end{aligned} \tag{15}$$

where G is a bulk free-electron Green's function:

$$G(\boldsymbol{q},\omega) = \left[\omega - E_{\boldsymbol{q}} + \mathrm{i}\eta\,\mathrm{sgn}(E_{\boldsymbol{q}} - E_{\mathrm{F}})\right]^{-1}. \tag{16}$$

Taking the dispersion $\omega = q^2/2$ and neglecting the recoil term for fast electrons leads to

$$G(\boldsymbol{q}_{\parallel}-\boldsymbol{q}'_{\parallel},q_{\perp}+v_{\perp},\omega-\omega') \simeq -(\omega' - \boldsymbol{q}_{\parallel}\cdot\boldsymbol{q}'_{\parallel} + q_{\perp}v_{\perp} - \mathrm{i}\eta)^{-1}. \tag{17}$$

The condition for an electron moving from the interior of a metal towards the surface is $v_\perp > 0$. The sign of the vertical velocity thus affects the analytic properties of the Green's function.

The local self-energies $\Sigma_{\rm in}(z)$, for the incoming wave, and $\Sigma_{\rm out}(z)$, for the outgoing wave, are determined from

$$\Sigma_{\rm in}(z|\boldsymbol{q}_\parallel, v_\perp)\mathrm{e}^{\mathrm{i}v_\perp z} - \Sigma_{\rm out}(z|\boldsymbol{q}_\parallel, v_\perp)\mathrm{e}^{-\mathrm{i}v_\perp z} = \int_{-\infty}^{0} \Sigma(z<0, z'<0|\boldsymbol{q}_\parallel)(\mathrm{e}^{\mathrm{i}v_\perp z'} - \mathrm{e}^{-\mathrm{i}v_\perp z'})\ \mathrm{d}z' \tag{18}$$

where the variable ω has been removed after taking the dispersion relation. By substituting equations (12)–(17) into the above equation and making the change of the variables $\boldsymbol{q}_\parallel \to \boldsymbol{v}_\parallel$, $\boldsymbol{q}'_\parallel \to \boldsymbol{q}_\parallel$, $\omega' \to \omega$, we get

$$\begin{aligned}\Sigma_{\rm in}(z|\boldsymbol{v}_\parallel, v_\perp)\mathrm{e}^{\mathrm{i}v_\perp z} - \Sigma_{\rm out}(z|\boldsymbol{v}_\parallel, v_\perp)\mathrm{e}^{-\mathrm{i}v_\perp z} \\ = (2\pi)^{-4}\int \mathrm{d}\boldsymbol{q}_\parallel \int_{-\infty}^{\infty} \mathrm{d}p\ \mathrm{d}\omega\ A(z|\boldsymbol{q}_\parallel, p, \omega)B(\boldsymbol{q}_\parallel, p, \omega|\boldsymbol{v}_\parallel, v_\perp)\end{aligned} \tag{19}$$

where

$$\begin{aligned}B(\boldsymbol{q}_\parallel, p, \omega|\boldsymbol{v}_\parallel, v_\perp) = \sum_{n=1,-1} n\mathrm{e}^{n\mathrm{i}v_\perp z}\int_{-\infty}^{\infty}\mathrm{d}q_\perp\ \mathrm{e}^{\mathrm{i}q_\perp z}G(\boldsymbol{v}_\parallel - \boldsymbol{q}_\parallel, q_\perp + nv_\perp, \tfrac{1}{2}q^2 - \omega) \\ \times\ \left[(q_\perp + p - \mathrm{i}\eta)^{-1} - (q_\perp - p + \mathrm{i}\eta)^{-1}\right].\end{aligned} \tag{20}$$

Equation (17) states that $G(q_\perp + v_\perp)$ is analytical in the upper half-plane of $q_\perp$ for $v_\perp > 0$. Because $z < 0$, the contour integration in the above equation should be carried out in the lower half-plane. Then, taking p as $-q_\perp$ in equation (19) and comparing the two sides of the equation for the incoming wave term $\exp(\mathrm{i}v_\perp z)$, we obtain finally

$$\Sigma_{\rm in}(z<0) = -\frac{\mathrm{i}}{(2\pi)^3}\int \mathrm{d}\boldsymbol{q}_\parallel \int_{-\infty}^{\infty}\mathrm{d}q_\perp\ \mathrm{d}\omega\ \mathrm{e}^{\mathrm{i}q_\perp z}\frac{A(z|\boldsymbol{q},\omega)}{\omega - \boldsymbol{q}\cdot\boldsymbol{v} - \mathrm{i}\eta} = \Sigma^{\rm b} + \Sigma^{\rm i}(z) + \Sigma^{\rm s}(z). \tag{21}$$

Hence, the self-energy of an electron moving towards the surface is made up of three terms. The first term, which is independent of z, describes the bulk excitation due to external charge:

$$\Sigma^{\rm b} = \frac{2}{(2\pi)^2}\int\frac{\mathrm{d}\boldsymbol{q}}{q^2}\int_0^\infty \mathrm{d}\omega\left(\frac{1}{\varepsilon(\boldsymbol{q},\omega)} - 1\right)\delta(\omega - \boldsymbol{q}\cdot\boldsymbol{v}) \tag{22}$$

where we have used the following property of the time-ordered dielectric function: $\varepsilon(\boldsymbol{q},\omega) = \varepsilon(-\boldsymbol{q},-\omega)$. The rest of the terms account for the surface effect. The second term, which is due to the image charge, is the boundary correction to the bulk term due to the presence of the surface:

$$\Sigma^{\rm i}(z) = -\frac{2\mathrm{i}}{(2\pi)^3}\int \mathrm{d}\boldsymbol{q}_\parallel\int_0^\infty\mathrm{d}\omega\int_{-\infty}^{\infty}\frac{\mathrm{d}q_\perp}{q^2\varepsilon(\boldsymbol{q},\omega)}\left(\frac{\mathrm{e}^{-2\mathrm{i}q_\perp z}}{\omega - \boldsymbol{q}\cdot\boldsymbol{v} - \mathrm{i}\eta} - \frac{\mathrm{e}^{2\mathrm{i}q_\perp z}}{\omega - \boldsymbol{q}\cdot\boldsymbol{v} + \mathrm{i}\eta}\right) \tag{23}$$

and the third one involving the surface dielectric function represents the surface excitation contributed by the surface charges:

$$\begin{aligned}\Sigma^{\rm s}(z) = \frac{\mathrm{i}}{2\pi^4}\int\mathrm{d}\boldsymbol{q}_\parallel\int_0^\infty\mathrm{d}\omega\ q_\parallel\varepsilon_{\rm s}(\boldsymbol{q}_\parallel,\omega)\int_{-\infty}^{\infty}\mathrm{e}^{\mathrm{i}q_\perp z}\ \frac{\mathrm{d}q_\perp}{q^2\varepsilon(\boldsymbol{q},\omega)} \\ \times\ \int_{-\infty}^{\infty}\frac{\mathrm{d}q_\perp}{q^2\varepsilon(\boldsymbol{q},\omega)}\left(\frac{\mathrm{e}^{-\mathrm{i}q_\perp z}}{\omega - \boldsymbol{q}\cdot\boldsymbol{v} - \mathrm{i}\eta} - \frac{\mathrm{e}^{\mathrm{i}q_\perp z}}{\omega - \boldsymbol{q}\cdot\boldsymbol{v} + \mathrm{i}\eta}\right).\end{aligned} \tag{24}$$

For the outgoing wave, $\exp(-\mathrm{i}v_\perp z)$, p should be replaced by $\pm q_\perp$ in equation (19) to make $\omega - \boldsymbol{q}_\parallel \cdot \boldsymbol{v}_\parallel \mp p v_\perp - \mathrm{i}\eta = \omega - \boldsymbol{q}\cdot\boldsymbol{v} - \mathrm{i}\eta$. One then finds the same expression for the self-energy $\Sigma_{\mathrm{out}}(z<0)$ as for the incoming wave. The values are, however, different, because the electron moves with actual vertical velocity $-v_\perp < 0$, except in the cases of $z = 0$ and of an electron trajectory parallel to the surface.

2.3. Zero barrier height

When the surface barrier is negligible, a moving electron travels without reflection at the surface. The surface Green's function takes the form

$$G_{\mathrm{s}}(zz'|\boldsymbol{q}_\parallel,\omega) = G(z-z'|\boldsymbol{q}_\parallel,\omega) = (2\pi)^{-1}\int_{-\infty}^{\infty} \mathrm{d}q_\perp\ G(\boldsymbol{q},\omega)\mathrm{e}^{\mathrm{i}q_\perp(z-z')} \tag{25}$$

and the self-energy satisfies

$$\Sigma(z|\boldsymbol{q}_\parallel, v_\perp)\mathrm{e}^{\mathrm{i}v_\perp z} = \int_{-\infty}^{\infty} \Sigma(zz'|\boldsymbol{q}_\parallel)\mathrm{e}^{\mathrm{i}v_\perp z'}\ \mathrm{d}z'. \tag{26}$$

Let us firstly consider the case where $z<0$. On using the relation

$$\int_{-\infty}^{\infty}\Phi(z<0,z'|\boldsymbol{q}_\parallel)\mathrm{e}^{-\mathrm{i}q_\perp z'}\ \mathrm{d}z' = \int_{-\infty}^{\infty}\mathrm{d}p\ \frac{A(z|\boldsymbol{q}_\parallel,p,\omega)}{\mathrm{i}(p-q_\perp)+\eta} - \frac{2\pi}{q_\parallel(q_\parallel+\mathrm{i}q_\perp)}\left\{\mathrm{e}^{q_\parallel z} - 2\varepsilon_{\mathrm{s}}(\boldsymbol{q}_\parallel,\omega)\frac{q_\parallel}{\pi}\int_{-\infty}^{\infty}\mathrm{e}^{\mathrm{i}q_\perp z}\ \frac{\mathrm{d}q_\perp}{q^2\varepsilon(\boldsymbol{q},\omega)}\right\} \tag{27}$$

in equation (26) and making the change of variables as before, it can be seen that the self-energy $\Sigma_{\mathrm{in}}(z<0)$ is identical to equation (21). The second term in the above equation due to $\Phi(z<0,z'>0)$ gives a vanishing contribution to the self-energy as is seen by carrying out contour integration of $q_\perp$ in lower half-plane.

When an electron is ejected into the vacuum ($z>0$, $v_\perp>0$), we can obtain the local self-energy from equation (26) as the sum $\Sigma_{\mathrm{out}}(z>0) = \Sigma_1(z) + \Sigma_2(z)$, where

$$\Sigma_1(z) = -\frac{1}{2\pi^2}\int \mathrm{d}\boldsymbol{q}_\parallel\ \frac{\mathrm{e}^{-2q_\parallel z}}{q_\parallel}\int_0^\infty \mathrm{d}\omega\ [1-2\varepsilon_{\mathrm{s}}(\boldsymbol{q}_\parallel,\omega)]\frac{q_\parallel v_\perp}{(\omega-\boldsymbol{q}_\parallel\cdot\boldsymbol{v}_\parallel)^2+(q_\parallel v_\perp)^2} \tag{28}$$

$$\begin{aligned}\Sigma_2(z) = \frac{\mathrm{i}}{(2\pi)^2}\int \mathrm{d}\boldsymbol{q}_\parallel\ \frac{\mathrm{e}^{-q_\parallel z}}{q_\parallel}\int_0^\infty \mathrm{d}\omega\ \Bigg\{&\left[\frac{\mathrm{e}^{-\mathrm{i}(\omega-\boldsymbol{q}_\parallel\cdot\boldsymbol{v}_\parallel)z/v_\perp}}{\omega-\boldsymbol{q}_\parallel\cdot\boldsymbol{v}_\parallel-\mathrm{i}q_\parallel v_\perp} - \mathrm{CC}\right]\\ &+[1-2\varepsilon_{\mathrm{s}}(\boldsymbol{q}_\parallel,\omega)]\left[\frac{\mathrm{e}^{-\mathrm{i}(\omega-\boldsymbol{q}_\parallel\cdot\boldsymbol{v}_\parallel)z/v_\perp}}{\omega-\boldsymbol{q}_\parallel\cdot\boldsymbol{v}_\parallel+\mathrm{i}q_\parallel v_\perp} - \mathrm{CC}\right]\\ &-2\varepsilon_{\mathrm{s}}(\boldsymbol{q}_\parallel,\omega)\frac{q_\parallel}{\pi}\int_{-\infty}^{\infty}\frac{\mathrm{d}q_\perp}{q^2\varepsilon(\boldsymbol{q},\omega)}\left[\frac{\mathrm{e}^{-\mathrm{i}(\omega-\boldsymbol{q}_\parallel\cdot\boldsymbol{v}_\parallel)z/v_\perp}}{\omega-\boldsymbol{q}\cdot\boldsymbol{v}-\mathrm{i}\eta} - \mathrm{CC}\right]\Bigg\}.\end{aligned} \tag{29}$$

$\Sigma_1(z)$ is equal to the self-energy for an electron incident onto the surface from the vacuum [14], $\Sigma_{\mathrm{in}}(z>0)$, and also agrees with a semiclassical result. $\Sigma_2(z)$, hence, vanishes for $v_\perp = 0$.

It is easy to verify that the continuity at the surface is guaranteed for both the cases of $U=0$ and $U=\infty$, where U stands for the barrier height:

$$\begin{aligned}\Sigma_{\mathrm{in}}(z=0^-;U=0) &= \Sigma_{\mathrm{out}}(z=0^+;U=0) = \Sigma_{\mathrm{in}}(z=0^-;U=\infty)\\ &= \Sigma_{\mathrm{out}}(z=0^-;U=\infty)\\ &= -\frac{1}{2\pi^2}\int\frac{\mathrm{d}\boldsymbol{q}}{q^2}\int_0^\infty\mathrm{d}\omega\ \delta(\omega-\boldsymbol{q}\cdot\boldsymbol{v})\\ &\quad+\frac{1}{\pi^2}\int\mathrm{d}\boldsymbol{q}_\parallel\int_0^\infty\mathrm{d}\omega\ \varepsilon_{\mathrm{s}}(\boldsymbol{q}_\parallel,\omega)\int_{-\infty}^{\infty}\frac{\mathrm{d}q_\perp}{q^2\varepsilon(\boldsymbol{q},\omega)}\ \delta(\omega-\boldsymbol{q}\cdot\boldsymbol{v}).\end{aligned} \tag{30}$$

2.4. A parallel trajectory

Formulae (21)–(24), (28)–(29) are valid for arbitrary take-off angle of the direction of movement of an electron with respect to the surface normal. Now we consider a specific case: $v_\perp = 0$, i.e., the trajectory parallel to the surface, corresponding to glancing detection geometry for scattering electrons. First, for an electron moving outside the solid with the velocity vector along the y-axis, $\Sigma_1(z)$ can be simplified using

$$\lim_{v_\perp \to 0} \frac{q_\parallel v_\perp}{(\omega - \boldsymbol{q}_\parallel \cdot \boldsymbol{v}_\parallel)^2 + (q_\parallel v_\perp)^2} = \pi \delta(\omega - \boldsymbol{q}_\parallel \cdot \boldsymbol{v}_\parallel) = \pi \delta(\omega - q_y v) \tag{31}$$

while $\Sigma_2(z)$ is equal to zero, guaranteeing that $\Sigma_{\text{in}}(z > 0) = \Sigma_{\text{out}}(z > 0)$. Defining the energy-loss cross-section $p(\omega)$ as

$$-2 \operatorname{Im} \Sigma(z) = v \int p(z|\omega)\ \mathrm{d}\omega \tag{32}$$

and

$$\varepsilon_n^{-1}(z|\boldsymbol{q}_\parallel, \omega) = \frac{q_\parallel}{\pi} \int_{-\infty}^{\infty} \cos(n q_\perp z)\ \frac{\mathrm{d}q_\perp}{q^2 \varepsilon(\boldsymbol{q}, \omega)} \tag{33}$$

it is easy to perform the integration over q_y and derive

$$p(z > 0|\omega) = \frac{2}{\pi v^2} \int_0^\infty \mathrm{d}q_x\ \frac{\mathrm{e}^{-2Qz}}{Q} \operatorname{Im}\left\{\frac{\varepsilon_0(Q, \omega) - 1}{\varepsilon_0(Q, \omega) + 1}\right\} \tag{34}$$

where $Q = \sqrt{q_x^2 + (\omega/v)^2}$.

Next, we consider the case where $z < 0$. The bulk term, equation (22), yields the bulk excitation cross-section in the form

$$p^{\text{b}}(\omega) = \frac{2}{\pi v^2} \int_0^\infty \frac{\mathrm{d}q_x}{Q} \operatorname{Im}\left\{\frac{-1}{\varepsilon_0(Q, \omega)}\right\}. \tag{35}$$

The surface excitation cross-section can also be easily obtained, considering that the parentheses in equations (23) and (24) reduce to the δ-function of equation (31):

$$p^{\text{i}}(z < 0|\omega) = \frac{2}{\pi v^2} \int_0^\infty \frac{\mathrm{d}q_x}{Q} \operatorname{Im}\left\{\frac{-1}{\varepsilon_2(z|Q, \omega)}\right\} \tag{36}$$

$$p^{\text{s}}(z < 0|\omega) = \frac{2}{\pi v^2} \int_0^\infty \frac{\mathrm{d}q_x}{Q} \operatorname{Im}\left\{\frac{2\varepsilon_0(Q, \omega)}{\varepsilon_1^2(z|Q, \omega)\,[1 + \varepsilon_0(Q, \omega)]}\right\}. \tag{37}$$

The total excitation cross-section is then $p = p^{\text{b}} + p^{\text{i}} + p^{\text{s}}$. These expressions reproduce the result obtained by Zabala and Echenique [8].

3. Plasmon excitation

3.1. The surface dielectric function and sum rules

Let us now look for the solution of the electron–surface inelastic interaction problem for a system described by the dielectric function [18]

$$\varepsilon(q, \omega) = 1 + \frac{\omega_p^2}{\omega_q^2 - \omega_p^2 - \omega(\omega + \mathrm{i}\gamma)}. \tag{38}$$

The system has a single plasmon with the energy ω_p and damping constant γ. ω_q denotes a dispersion relation:

$$\omega_q^2 = \omega_{\text{g}}^2 + \omega_p^2 + \beta^2 q^2 + q^4/4 \tag{39}$$

where the energy ω_g accounts for the band gap in a semiconductor.

The surface dielectric function defined by equation (4) can then be derived from the residues of the integral. The poles of $\varepsilon^{-1}(q,\omega)$ in the plane of $q_\perp$ are determined by

$$\omega_g^2 + \omega_p^2 - \omega(\omega + i\gamma) + \beta^2 q^2 + q^4/4 = 0. \tag{40}$$

There are four roots, $(\pm q_1, \pm q_2)$, for the solution of this equation, where q_1 and q_2 denote two poles in the upper half-plane of $q_\perp$: $\arg(q_1) \in [0, \pi/2]$; $\arg(q_2) \in [\pi/2, \pi]$. Hence, we found

$$\varepsilon_s^{-1}(q_\parallel, \omega) = 1 + \varepsilon^{-1}(\omega) - i\frac{4q_\parallel \omega_p^2}{q_1^2 - q_2^2}\left[\frac{1}{q_1(q_1^2 + q_\parallel^2)} - \frac{1}{q_2(q_2^2 + q_\parallel^2)}\right] \tag{41}$$

where $\varepsilon(\omega)$ stands for $\varepsilon(0,\omega)$.

By finding four poles of the bulk energy-loss function,

$$\mathrm{Im}\left\{\frac{-1}{\varepsilon(q,\omega)}\right\} = \frac{\omega\gamma\omega_p^2}{(\omega^2 - \omega_q^2)^2 + (\omega\gamma)^2} \tag{42}$$

in the ω-plane, $(\pm\omega_1, \pm\omega_1^*)$, where $\omega_1(q) = \sqrt{\omega_q^2 - (\gamma/2)^2} + i\gamma/2$, we may verify the bulk f-sum rule:

$$\mu_1^b(q) = \int_0^\infty \omega\,\mathrm{Im}\left\{\frac{-1}{\varepsilon(q,\omega)}\right\}\,d\omega = \frac{1}{2}\omega_p^2\gamma\frac{\pi i}{\omega_1 - \omega_1^*} = \frac{\pi}{2}\omega_p^2 \tag{43}$$

and the perfect-screening sum rule:

$$\mu_{-1}^b = \lim_{q\to 0}\int_0^\infty \frac{1}{\omega}\,\mathrm{Im}\left\{\frac{-1}{\varepsilon(q,\omega)}\right\}\,d\omega = \frac{1}{2}\omega_p^2\gamma\frac{\pi i}{\omega_1 - \omega_1^*}\frac{1}{|\omega_1(0)|^2} = \frac{\pi}{2}\left(\frac{\omega_p}{\omega_0}\right)^2 \simeq \frac{\pi}{2} \tag{44}$$

where $\omega_0 = \omega_{q=0} = \sqrt{\omega_g^2 + \omega_p^2}$, for $\omega_g \ll \omega_p$.

Making the change $\omega_q^2 \to \omega_q^2 - \omega_p^2$, the expression for $\mathrm{Im}\{-1/\varepsilon(q,\omega)\}$ in equation (42) becomes $\mathrm{Im}\{\varepsilon(q,\omega)\}$, and the corresponding bulk sum rules [19] are

$$\nu_1^b(q) = \int_0^\infty \omega\,\mathrm{Im}\{\varepsilon(q,\omega)\}\,d\omega = \frac{\pi}{2}\omega_p^2 \tag{45}$$

$$\nu_{-1}^b = \lim_{q\to 0}\int_0^\infty \frac{1}{\omega}\,\mathrm{Im}\{\varepsilon(q,\omega)\}\,d\omega = \frac{\pi}{2}\frac{\omega_p^2}{\omega_g^2}. \tag{46}$$

It is natural that the surface dielectric function would also satisfy certain surface sum rules. From the definitions given as equation (4) and equation (41), it is quite easy to see that the surface energy-loss function satisfies the surface f-sum rule

$$\mu_1^s(q_\parallel) = \int_0^\infty \omega\,\mathrm{Im}\left\{\frac{-1}{\varepsilon_s(q_\parallel,\omega)}\right\}\,d\omega = \frac{\pi}{2}\omega_p^2 = \mu_1^b(q). \tag{47}$$

Using equation (41), we have

$$\mu_{-1}^s = \lim_{q_\parallel\to 0}\int_0^\infty \frac{1}{\omega}\,\mathrm{Im}\left\{\frac{-1}{\varepsilon_s(q_\parallel,\omega)}\right\}\,d\omega = \int_0^\infty \frac{1}{\omega}\,\mathrm{Im}\left\{\frac{-1}{\varepsilon(\omega)}\right\}\,d\omega = \mu_{-1}^b. \tag{48}$$

Two counterpart surface sum rules for $S(q_\parallel,\omega) = 2\pi^{-1}\,\mathrm{Im}\{\varepsilon_s(q_\parallel,\omega)\}$ have been given by Gumhalter [20]. To verify them, we may note that

$$\mathrm{Im}\{\varepsilon_s(0,\omega)\} = \frac{1}{2}\frac{\omega\gamma\omega_s^2}{(\omega^2 - \omega_0^2 + \omega_s^2)^2 + (\omega\gamma)^2} \tag{49}$$

where $\omega_s = \omega_p/\sqrt{2}$. Comparing this equation with equation (42) leads to

$$\nu_{-1}^s = \lim_{q_\parallel \to 0} \int_0^\infty \frac{1}{\omega} \operatorname{Im}\left\{\varepsilon_s(q_\parallel, \omega)\right\}\ \mathrm{d}\omega = \frac{\pi}{4}\frac{\omega_s^2}{\omega_s^2 + \omega_g^2} \simeq \frac{\pi}{4} \tag{50}$$

$$\nu_1^s(q_\parallel = 0) = \int_0^\infty \omega \operatorname{Im}\left\{\varepsilon_s(0, \omega)\right\}\ \mathrm{d}\omega = \frac{\pi}{4}\omega_s^2. \tag{51}$$

In fact, equation (51) holds generally for arbitrary $q_\parallel$:

$$\nu_1^s(q_\parallel) = \int_0^\infty \omega \operatorname{Im}\left\{\varepsilon_s(q_\parallel, \omega)\right\}\ \mathrm{d}\omega = \frac{\pi}{4}\omega_s^2 \tag{52}$$

which may be tested numerically.

3.2. The formula for the self-energy

The expression for the electron self-energy may be further simplified by integrating out the $q_\perp$-component using the dielectric function (38). By the argument used to derive equation (41), we obtain

$$H(q_\parallel, \omega) \equiv \frac{q_\parallel}{\pi}\int_{-\infty}^{\infty} \mathrm{e}^{\mathrm{i}q_\perp z}\ \frac{\mathrm{d}q_\perp}{q^2\varepsilon(q,\omega)} = \frac{\mathrm{e}^{q_\parallel z}}{\varepsilon(\omega)} - \mathrm{i}\frac{4q_\parallel\omega_p^2}{q_1^2 - q_2^2}\left[\frac{\mathrm{e}^{-\mathrm{i}q_1 z}}{q_1(q_1^2 + q_\parallel^2)} - \frac{\mathrm{e}^{-\mathrm{i}q_2 z}}{q_2(q_2^2 + q_\parallel^2)}\right] \tag{53}$$

and

$$\begin{aligned} F_n^\pm(\boldsymbol{q}_\parallel, \omega|\boldsymbol{v}) &\equiv \frac{q_\parallel}{\pi}\int_{-\infty}^{\infty}\frac{\mathrm{d}q_\perp}{q^2\varepsilon(q,\omega)}\ \frac{\mathrm{e}^{\pm\mathrm{i}nq_\perp z}}{\omega - \boldsymbol{q}\cdot\boldsymbol{v} \pm \mathrm{i}\eta} \\ &= \frac{\mathrm{e}^{nq_\parallel z}}{\varepsilon(\omega)}\frac{1}{\omega - \boldsymbol{q}_\parallel\cdot\boldsymbol{v}_\parallel \pm \mathrm{i}q_\parallel v_\perp} - \mathrm{i}\frac{4q_\parallel\omega_p^2}{q_1^2 - q_2^2}\left[\frac{\mathrm{e}^{-\mathrm{i}nq_1 z}}{q_1(q_1^2 + q_\parallel^2)}\frac{1}{\omega - \boldsymbol{q}_\parallel\cdot\boldsymbol{v}_\parallel \pm q_1 v_\perp}\right. \\ &\quad \left. - \frac{\mathrm{e}^{-\mathrm{i}nq_2 z}}{q_2(q_2^2 + q_\parallel^2)}\frac{1}{\omega - \boldsymbol{q}_\parallel\cdot\boldsymbol{v}_\parallel \pm q_2 v_\perp}\right]. \end{aligned} \tag{54}$$

Moreover, the polar angles of $\boldsymbol{q}_\parallel$ may be integrated out to give

$$\begin{aligned} P_n^\pm(q_\parallel, \omega|\boldsymbol{v}) &\equiv \frac{1}{2\pi}\int_0^{2\pi} F_n^\pm(\boldsymbol{q}_\parallel, \omega|\boldsymbol{v})\ \mathrm{d}\varphi \\ &= \frac{\mathrm{e}^{nq_\parallel z}}{\varepsilon(\omega)}Q_0(\pm\mathrm{i}q_\parallel) - \mathrm{i}\frac{4q_\parallel\omega_p^2}{q_1^2 - q_2^2}\left[\frac{\mathrm{e}^{-\mathrm{i}nq_1 z}}{q_1(q_1^2 + q_\parallel^2)}Q_0(\pm q_1)\right. \\ &\quad \left. - \frac{\mathrm{e}^{-\mathrm{i}nq_2 z}}{q_2(q_2^2 + q_\parallel^2)}Q_0(\pm q_2)\right] \end{aligned} \tag{55}$$

and

$$\begin{aligned} R^\pm(q_\parallel, \omega|\boldsymbol{v}) &\equiv \frac{1}{2\pi}\int_0^{2\pi} F_0^\pm(\boldsymbol{q}_\parallel, \omega|\boldsymbol{v})\exp\left\{\pm\mathrm{i}(\omega - \boldsymbol{q}_\parallel\cdot\boldsymbol{v}_\parallel)z/v_\perp\right\}\ \mathrm{d}\varphi \\ &= \frac{1}{\varepsilon(\omega)}Q_1^\pm(\pm\mathrm{i}q_\parallel) - \mathrm{i}\frac{4q_\parallel\omega_p^2}{q_1^2 - q_2^2}\left[\frac{1}{q_1(q_1^2 + q_\parallel^2)}Q_1^\pm(\pm q_1)\right. \\ &\quad \left. - \frac{1}{q_2(q_2^2 + q_\parallel^2)}Q_1^\pm(\pm q_2)\right] \end{aligned} \tag{56}$$

where

$$Q_n^{\pm}(q) \equiv \frac{1}{2\pi}\int_0^{2\pi} \mathrm{d}\varphi \ \frac{\exp\left\{\pm \mathrm{i}n(\omega - \boldsymbol{q}_\parallel \cdot \boldsymbol{v}_\parallel)z/v_\perp\right\}}{\omega - \boldsymbol{q}_\parallel \cdot \boldsymbol{v}_\parallel + qv_\perp}. \tag{57}$$

Though Q_1 can be expanded to a series involving Bessel functions, we prefer to use a direct numerical integration routine. Q_0 is written out explicitly as

$$Q_0^{\pm}(q) = -\frac{2}{q_\parallel v_\parallel}\frac{1}{\zeta_1 - \zeta_2}\left[\theta(1 - |\zeta_1|) - \theta(1 - |\zeta_2|)\right] \tag{58}$$

where $\zeta_{1,2}(q)$ are the solutions of the equation $\zeta^2 - 2(q_\parallel v_\parallel)^{-1}(\omega + qv_\perp)\zeta + 1 = 0$. $\theta(x)$ is the Heaviside step function.

Finally, the surface self-energy terms for $z < 0$ in equations (23) and (24) become, respectively,

$$\Sigma^{\mathrm{i}}(z) = -\frac{\mathrm{i}}{2\pi}\int_0^{E-E_\mathrm{F}} \mathrm{d}\omega \int_0^{\infty} \mathrm{d}q_\parallel \ (P_2^- - P_2^+) \tag{59}$$

$$\Sigma^{\mathrm{s}}(z) = \frac{\mathrm{i}}{\pi}\int_0^{E-E_\mathrm{F}} \mathrm{d}\omega \int_0^{\infty} \mathrm{d}q_\parallel \ \varepsilon_\mathrm{s}(q_\parallel, \omega)H(q_\parallel, \omega)(P_1^- - P_1^+) \tag{60}$$

where E is electron kinetic energy. The bulk term is reduced by integrating over $\boldsymbol{q}$ to give

$$\Sigma^{\mathrm{b}}(z) = \frac{2\omega_p^2}{\pi v}\int_0^{E-E_\mathrm{F}} \frac{\mathrm{d}\omega}{q_1^2 - q_2^2}\left\{\frac{1}{q_1^2 + q_\parallel^2}\ln\left[\frac{q^2}{q^2 - (q_1^2 + q_\parallel^2)}\right] - \frac{1}{q_2^2 + q_\parallel^2}\ln\left[\frac{q^2}{q^2 - (q_2^2 + q_\parallel^2)}\right]\right\}\Bigg|_{\omega/v}^{\infty}. \tag{61}$$

Using $Q_0(-\mathrm{i}q_\parallel) = \left[Q_0(\mathrm{i}q_\parallel)\right]^*$ and $Q_1^-(-\mathrm{i}q_\parallel) = \left[Q_1^+(\mathrm{i}q_\parallel)\right]^*$, the self-energy terms for $z > 0$ may be written as

$$\Sigma_1(z) = \frac{1}{\pi}\int_0^{E-E_\mathrm{F}} \mathrm{d}\omega \int_0^{\infty} \mathrm{d}q_\parallel \ \mathrm{e}^{-2q_\parallel z}(1 - 2\varepsilon_\mathrm{s})\,\mathrm{Im}\{Q_0(\mathrm{i}q_\parallel)\} \tag{62}$$

$$\Sigma_2(z) = \frac{1}{\pi}\int_0^{E-E_\mathrm{F}} \mathrm{d}\omega \int_0^{\infty} \mathrm{d}q_\parallel \ \mathrm{e}^{-q_\parallel z}[\mathrm{Im}\{Q_1^+(\mathrm{i}q_\parallel)\} - (1 - 2\varepsilon_\mathrm{s})\,\mathrm{Im}\{Q_1^-(\mathrm{i}q_\parallel)\} - \mathrm{i}\varepsilon_\mathrm{s}(R^- - R^+)]. \tag{63}$$

3.3. Numerical calculation results

Although Flores and Garcia-Moliner gave the quantum expression for the self-energy for an electron penetrating through the surface from the vacuum side many years ago, numerical estimates of the surface effects based on this theory are still lacking. The complex form of the resulting expression has prevented it from being put into practical use. It is thus crucial to perform numerical calculations in order to observe the various aspects of the theory.

Considering that equation (38) models the dielectric response for a nearly free-electron material, we choose Si as the example on which to carry out a numerical investigation of the self-energy and inelastic scattering cross-section. Figure 1 compares the energy-loss functions, $\mathrm{Im}\{-1/\varepsilon(\omega)\}$, derived from the optical data and the present theoretical model, with the parameters $\omega_p = 16.64$ eV, $\omega_\mathrm{g} = 1.17$ eV and $\gamma = 4$ eV.

In our previous study [21], an optical data model with the dispersion equation $\omega_q = \omega_p + \frac{1}{2}q^2$ was adopted. To allow comparison of the present model calculation with the previous results, the same dispersion relation was used—that is, we set $\beta = \sqrt{\omega_p}$ in

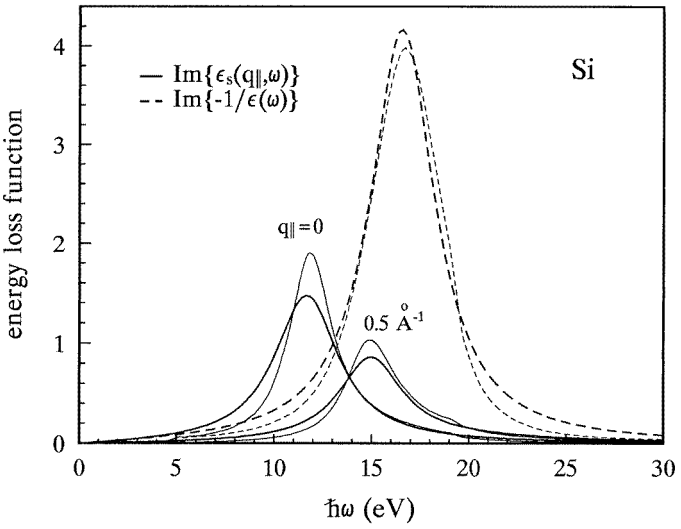

Figure 1. A comparison of the surface energy-loss function (solid lines) with the bulk energy-loss function (dashed lines). The thin and thick lines represent, respectively, the calculation results obtained using an optical data model [21] and the present dielectric function, equation (38).

equation (39). Figure 1 shows the surface energy-loss function, $\mathrm{Im}\{\varepsilon_s(q_\parallel,\omega)\}$, for two representative values of $q_\parallel$. The intensity of the bulk plasmon loss peak obtained from the model is slightly higher than that deduced from optical data and the surface plasmon peak is correspondingly lower. However, the surface plasmon dispersion is, as expected, similar.

We scale the differential self-energy $\bar{\Sigma}(\omega)$ and the double-differential self-energy $\bar{\Sigma}(q_\parallel,\omega)$ so that

$$-2v^{-1}\Sigma(z)=\bar{\Sigma}(z)=\int \mathrm{d}\omega\ \bar{\Sigma}(z|\omega)=\int \mathrm{d}\omega\int_0^\infty \mathrm{d}q_\parallel\ \bar{\Sigma}(z|q_\parallel,\omega). \tag{64}$$

Let $\bar{\Sigma}=b+\mathrm{i}p$; the real part b and imaginary part p represent, respectively, the scaled image potential energy and the energy-loss cross-section. Because the double-differential self-energy depends on many variables including the horizontal momentum transfer, energy loss, depth, direction of movement and kinetic energy of an electron, we will only analyse certain aspects in the following.

Figure 2(a) shows a plot of the real and imaginary parts of $\bar{\Sigma}(z<0|q_\parallel,\omega)$ as functions of ω. It can be seen that the image charge contributes positively to p in the bulk plasmon energy loss; the surface charges set up an energy-loss mechanism via surface plasmon excitation and reduce the scattering probability of bulk plasmon excitation. The real part behaves like a differential of the imaginary part in shape. It should be kept in mind that the sum of the image charge term and the surface charge term is just the net surface effect in the case of an electron inside the medium, and the bulk term should be added in order to evaluate the total effect. When the electron is emitted into the vacuum ($z>0$), only the surface effect remains. Figure 2(b) indicates that p_2 and p_1 are, respectively, the positive and negative components of the energy-loss cross-section having a single peak at the surface plasmon energy. From equation (28), the classical self-energy for an electron approaching the surface from the vacuum is $-(b_1+\mathrm{i}p_1)$.

The z-dependence (not shown here) of $\bar{\Sigma}(z|q_\parallel,\omega)$ shows that the surface effect is the most pronounced at $z=0$ and vanishes for $z\to\pm\infty$. The trend of the variation will be

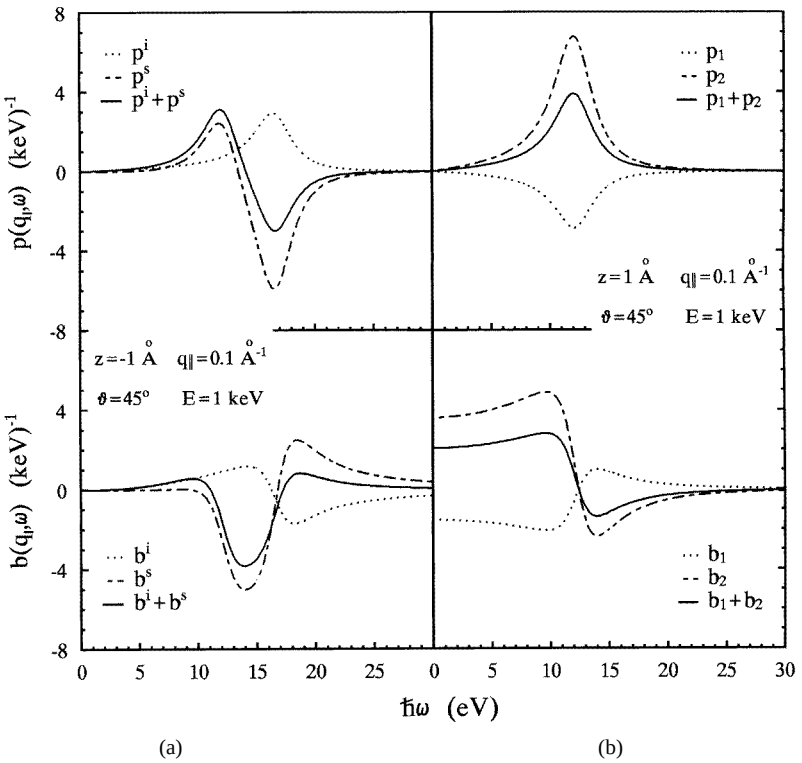

Figure 2. The double-differential self-energy as a function of ω at the given values of the horizontal wave vector $q_\parallel$, distance from the surface z, take-off angle ϑ and kinetic energy E. b and p are respectively the real and imaginary parts of the scaled self-energy, equation (64). The superscripts i and s refer to equations (59) and (60) for $z < 0$, and subscripts 1 and 2 to (62) and (63) for $z > 0$, respectively.

seen later from the perspective plot of $\bar{\Sigma}(\omega)$ versus z and ω.

Figures 3 and 4 show perspective plots of $\bar{\Sigma}(q_\parallel, \omega)$ for an electron inside the medium and in the vacuum, respectively. The peak positions of the surface plasmon and bulk plasmon in figure 3(a) are determined by the intersection of the plasmon dispersion and the resonant condition for plasmon excitation. This is what the term $(\omega - \boldsymbol{q}_\parallel \cdot \boldsymbol{v}_\parallel \pm q_{1,2} v_\perp)^{-1}$ implies in equation (54). In the case of an electron moving parallel to the surface, the dispersion effect involved in the imaginary part of the term diminishes and the term becomes $\delta(\omega - q_\parallel v)$—the matching of the phase velocity of the plasmon with the electron velocity.

For $z > 0$, only the surface plasmon excitation peak remains in figure 4(a). In the case of an electron moving normal to the surface, the analysis is simple: $Q_0(\mathrm{i}q_\parallel)$ becomes $(\omega + \mathrm{i}q_\parallel v)^{-1}$ whose imaginary part reaches a maximum at $\omega \to 0$ and $q_\parallel \to 0$ and extends along the line $\omega = q_\parallel v$. This factor, together with the exponential decay factor in $q_\parallel$ and the dispersion involved in $\mathrm{Im}\{\varepsilon_s(q_\parallel, \omega)\}$ governs the shape of p_1 as described by equation (62).

Figure 5 shows the variation of $\bar{\Sigma}(q_\parallel, \omega)$ with ω and take-off angle, θ, defined as the angle between the velocity vector and the surface normal. A large variation is found at the bulk plasmon energy and for the glancing condition $\theta \to \pi/2$. It is interesting to note that, for an electron moving outside the medium, there is still a small possibility for bulk plasmon excitation due solely to a surface effect if the electron is quite near to the surface.

Figure 6 shows the variation of the imaginary part of the differential self-energy, the

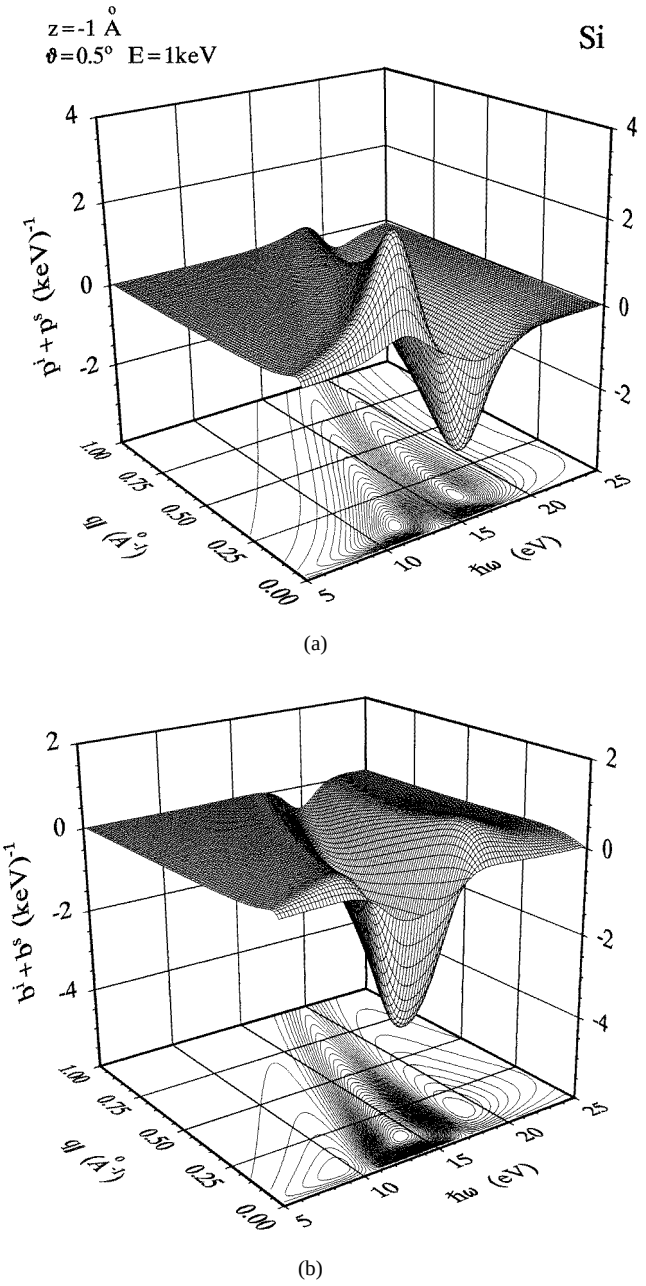

Figure 3. A perspective view of the double-differential self-energy as a function of ω and $q_\parallel$ for $z = -1$ Å. (a) The imaginary-part term $p^{\mathrm{i}} + p^{\mathrm{s}}$. (b) The real-part term $b^{\mathrm{i}} + b^{\mathrm{s}}$. The superscripts i and s refer to equations (59) and (60) respectively.

energy-loss distribution of electrons, with the distance from the surface. The transition from the bulk plasmon excitation mode to the surface plasmon excitation mode as the electron leaves the surface is clearly seen. The surface plasmon excitation is then the most probable at $z = 0$. The calculation of the energy-loss distribution of protons travelling parallel to

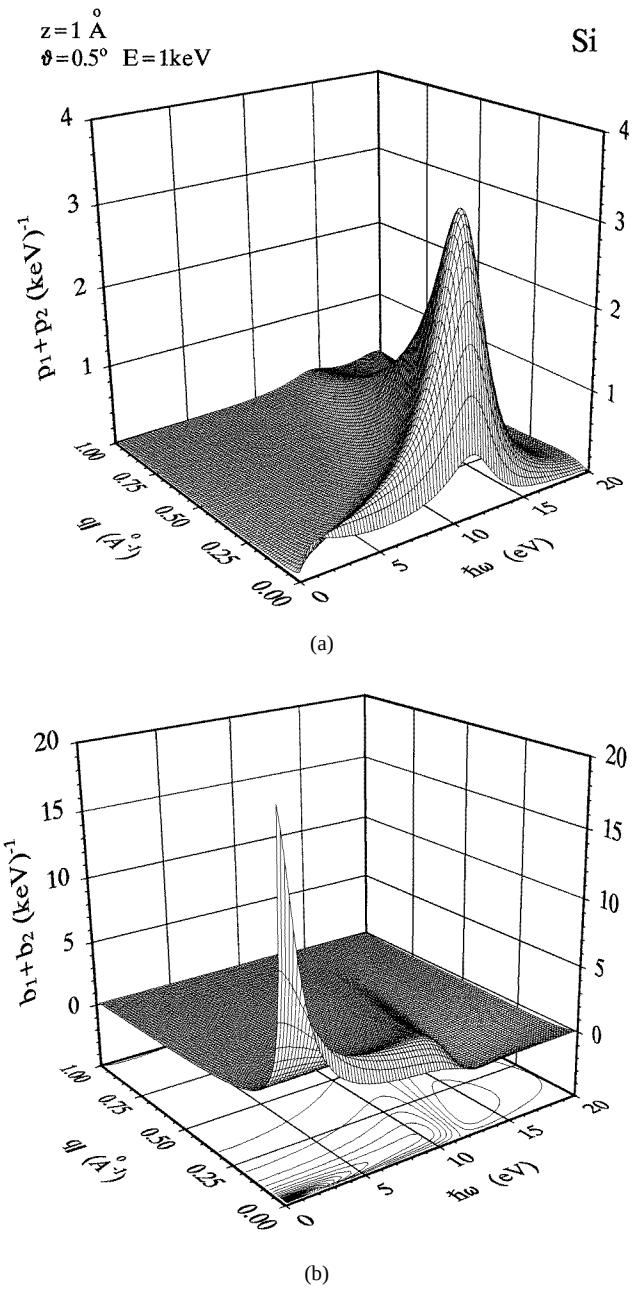

Figure 4. A perspective view of the double-differential self-energy, as a function of ω and $q_\parallel$ for $z = 1$ Å. (a) The imaginary-part term $p_1 + p_2$. (b) The real-part term $b_1 + b_2$. The subscripts 1 and 2 refer to equations (62) and (63) respectively.

an Al surface [10] has shown a similar behaviour, except that the position of the most probable surface plasmon excitation is at the electronic surface which was set at some distance from the geometrical surface. The effective surface excitation region extends into both the vacuum and the solid, to a distance about v/ω. The vacuum region contributes

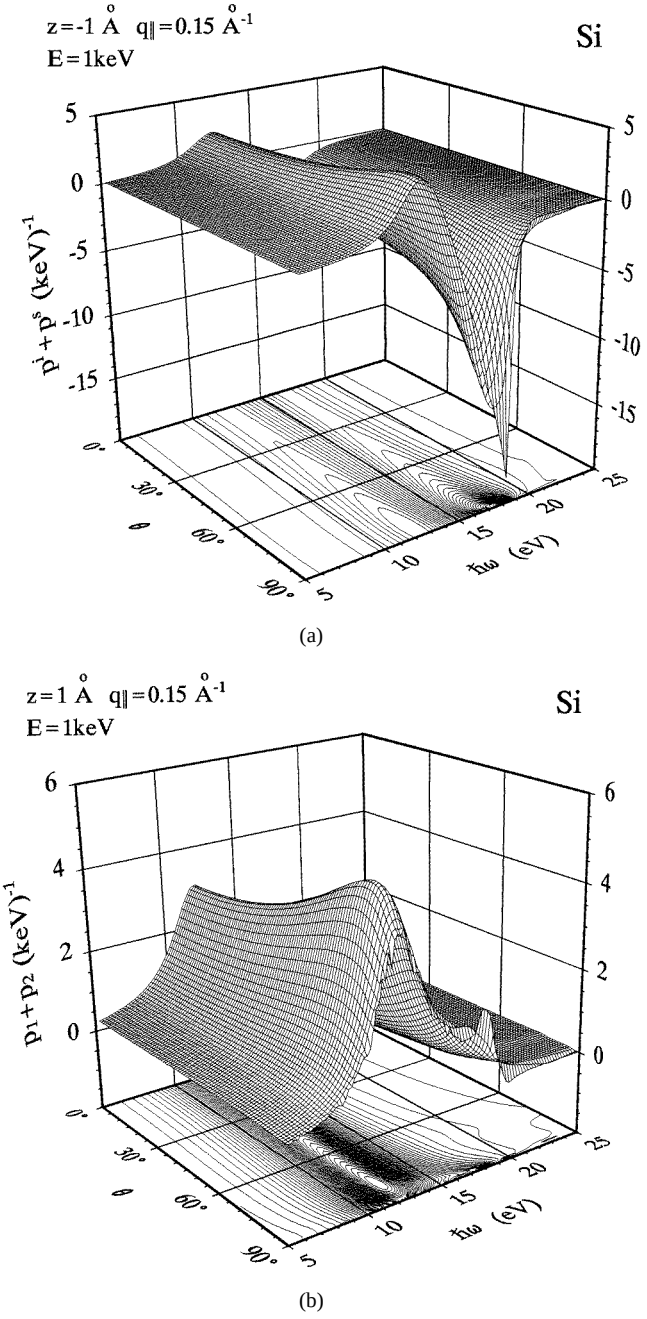

Figure 5. A perspective view of the imaginary part of the double-differential self-energy as a function of ω and θ: (a) for $z < 0$, calculated from equations (59) and (60); (b) for $z > 0$, calculated from equations (62) and (63).

almost half of the total energy-loss process; any theory ignoring this point [11] considerably underestimates the surface contributions. The present calculation scheme for the electron energy-loss distribution, with the full knowledge of the dependency on the kinetic energy,

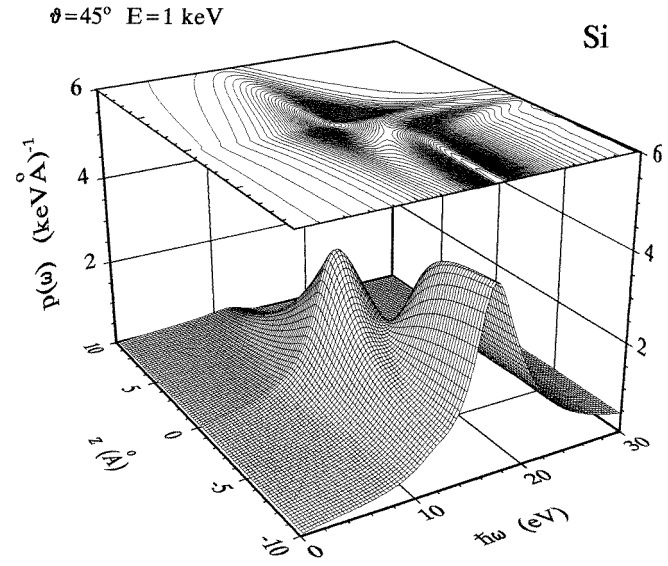

Figure 6. A perspective view of the imaginary part of the differential self-energy as a function of ω and z.

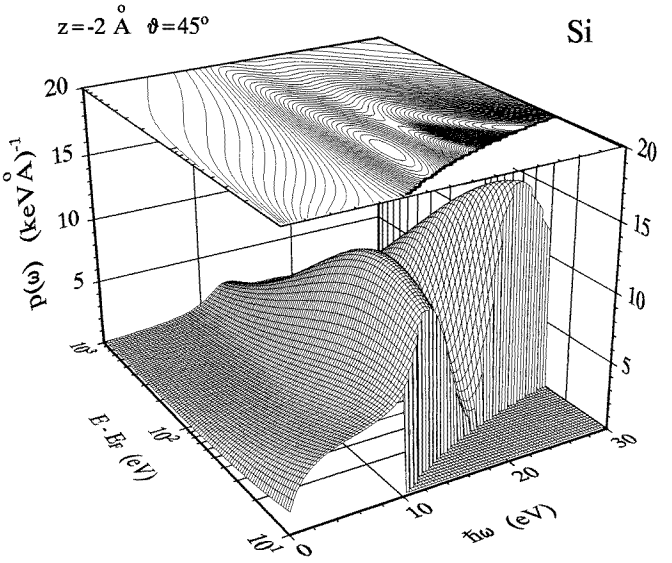

Figure 7. A perspective view of the imaginary part of the differential self-energy as a function of ω and E. A cut-off is imposed at $\omega = E - E_F$.

take-off angle and depth, should be useful in theoretical investigations in surface chemical analysis; for example, quantitative reflection electron energy-loss spectroscopy analysis can then be carried out by analysing the shape of the loss spectrum instead of by simple peak position analysis [23].

The kinetic energy dependency of the energy-loss distribution is shown by figure 7.

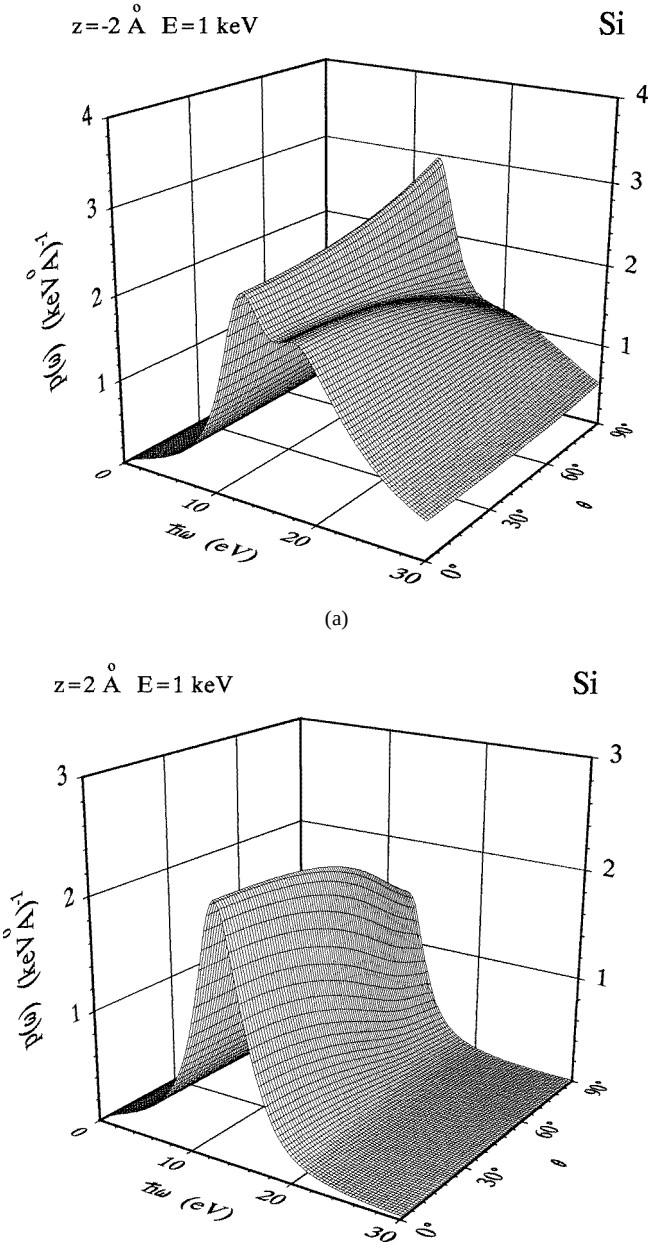

Figure 8. A perspective view of the imaginary part of the differential self-energy as a function of ω and θ. (a) $z < 0$. (b) $z > 0$.

A non-monotonic variation is found. For a specific value of the excitation energy ω, the energy dependence of the excitation function is analogous to the ionization cross-section having a maximum at an overvoltage ratio E/ω around 2.

Figure 8 shows the angular dependency of the energy-loss distribution. A smooth change

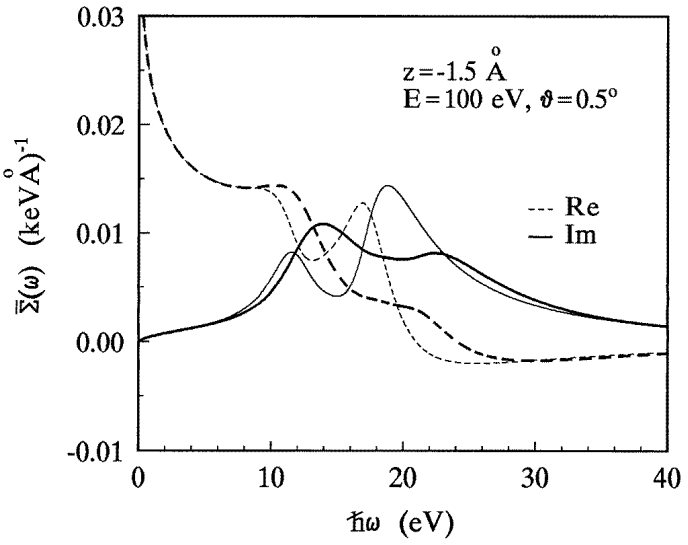

(a)

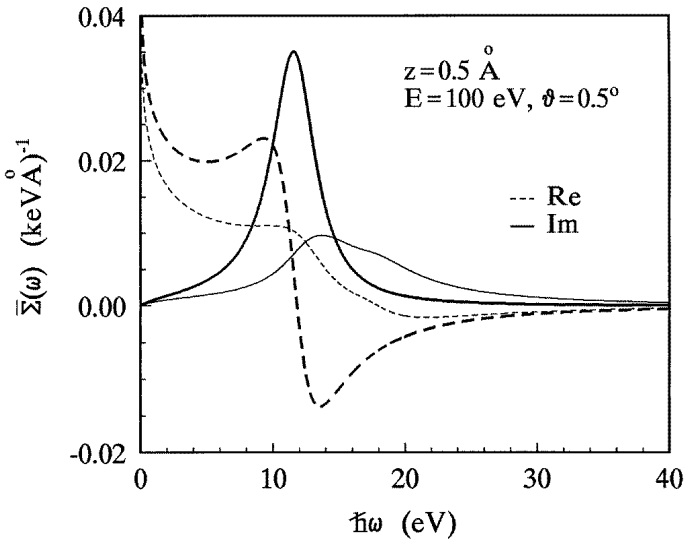

(b)

Figure 9. A comparison of the complex differential self-energies obtained from the calculations using dispersive (thick lines) and non-dispersive (thin lines) dielectric functions. (a) $z < 0$. (b) $z > 0$.

with take-off angle is found: for $z < 0$, the excitation probability of the surface plasmon increases with θ while that of the bulk plasmon decreases; for $z > 0$, a larger θ-value lowers the surface plasmon excitation probability.

To see how the plasmon dispersion affects the differential self-energy, a comparison has been made between the dispersive and non-dispersive dielectric function formulations in figure 9. The non-dispersive dielectric function $\varepsilon(\omega)$ is obtained by omitting the dispersion

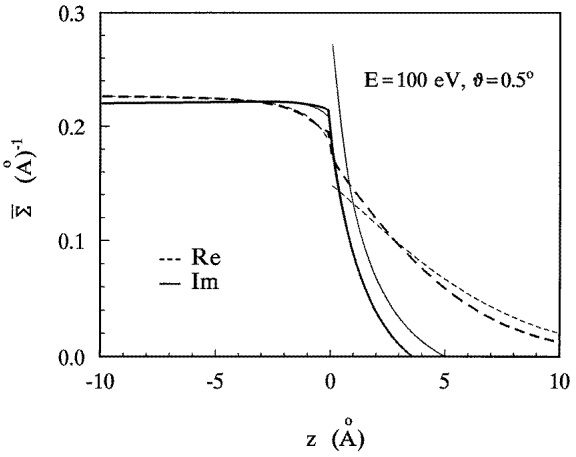

Figure 10. A comparison of the z-dependence of the complex self-energies obtained from the calculations using dispersive (thick lines) and non-dispersive (thin lines) dielectric functions.

in equation (38). Then, the terms involving $q_{1,2}$-factors in equations (41) and (53)–(56) should be neglected. It can be seen that the dispersive calculation result for $\mathrm{Im}\bar{\Sigma}(\omega)$ differs significantly from the non-dispersive one. In particular, for $z > 0$, the surface plasmon peak in the non-dispersive energy-loss distribution has not been predicted correctly.

Figure 10 shows the comparison between the dispersive and non-dispersive dielectric function formulations for the calculated complex electron self-energy, $\bar{\Sigma}(z)$, for plasmons. It is obvious that the non-dispersive calculation yields a divergent imaginary part of the self-energy for $z \to 0^+$, as found previously [5]. The non-dispersive real part of the self-energy, the image potential, is finite at $z \to 0^+$ [5] and is closer to the classical image potential, $-1/4z$ for $z \to \infty$, than the dispersive result. Note that the scaled image potential should be positive. The dispersive self-energy is continuous at $z = 0$ and decreases rapidly to zero as $z \to \infty$. The tendency of the change with z is quite reasonable and agrees qualitatively with other theories [5, 22].

4. Conclusions

In conclusion, we have derived an expression for the self-energy of a fast charged particle escaping from a solid to a vacuum for arbitrary take-off angle in terms of an arbitrary bulk dielectric function $\varepsilon(\boldsymbol{q}, \omega)$. The imaginary parts of equations (23), (24) and (28), (29) provide a detailed knowledge of the surface excitation cross-section including the dependence on the distance from the surface, kinetic energy and velocity vector of the particles in addition to the dependence on the energy loss and momentum transfer from the particle to medium. This knowledge will be useful for analysing the energy-loss spectrum in surface electron spectroscopies.

A Drude–Lindhard model bulk dielectric function $\varepsilon(\boldsymbol{q}, \omega)$ for describing a free-electron-like material is adopted to obtain a computable scheme for analysing the excitation processes of surface and bulk plasmon modes. A numerical calculation for Si has been performed to demonstrate how the complex self-energy changes with the distance from the surface, kinetic energy and take-off angle.

Acknowledgments

This work was supported in part by the National Natural Science Foundation of China, the Foundation for High Performance Computing and the Chinese Academy of Science through the grants CAS Presidential Foundation and *Liu Xue Hui Guo Ren Yuan Ze You Zi Zhu*. Some of the data presented here were calculated using a parallel computer, Dawn-1000, at the High Performance Computing Centre at Hefei.

References

[1] Ding Z J and Shimizu R 1995 *Surf. Sci.* **336** 397
[2] Ding Z J, Shimizu R and Goto K 1996 *Appl. Surf. Sci.* **100/101** 15
[3] Ferrell T L, Echenique P M and Ritchie R H 1979 *Solid State Commun.* **32** 419
[4] Nunez R, Echenique P M and Ritchie R H 1980 *J. Phys. C: Solid State Phys.* **13** 4229
[5] Echenique P M, Ritchie R H, Barberan N and Inkson J 1981 *Phys. Rev.* B **23** 6486
[6] Gras-Marti A, Echenique P M and Ritchie R H 1986 *Surf. Sci.* **173** 310
[7] Echenique P M, Bausells J and Rivacoba A 1987 *Phys. Rev.* B **35** 1521
[8] Zabala N and Echenique P M 1990 *Ultramicroscopy* **32** 327
[9] Yubero F and Tougaard S 1992 *Phys. Rev.* B **46** 2486
[10] Juaristi J I, Garcia de Abajo F J and Echenique P M 1996 *Phys. Rev.* B **53** 13 839
[11] Tung C J, Chen Y F, Kwei C M and Chou T L 1994 *Phys. Rev.* B **49** 16 684
[12] Chen Y F 1995 *J. Vac. Sci. Technol.* A **13** 2665
[13] Yubero F, Sanz J M, Ramskov B and Tougaard S 1996 *Phys. Rev.* B **53** 9719
[14] Flores F and Garcia-Moliner F 1979 *J. Phys. C: Solid State Phys.* **12** 907
[15] Ritchie R H and Marusak A L 1966 *Surf. Sci.* **4** 234
[16] Garcia-Moliner F and Flores F 1979 *Introduction to the Theory of Solid Surfaces* (Cambridge: Cambridge University Press)
[17] Flores F and Garcia-Moliner F 1984 *Surface Excitations* ed V M Agranovich and R Loudon (Amsterdam: Elsevier) p 441
[18] Echenique P M, Ritchie R H, and Brandt W 1979 *Phys. Rev.* B **20** 2567
[19] Mahan G D 1981 *Many Particle Physics* (New York: Plenum) p 459
[20] Gumhalter B 1975 *J. Physique* **38** 1117
[21] Ding Z J 1997 *Phys. Rev.* B **55** 9999
[22] Echenique P M, and Pendry J B 1990 *Prog. Surf. Sci.* **32** 111
[23] Kurokawa A and Shimizu R 1989 *Surf. Sci.* **207** 460